ORIGINAL ARTICLE

CrossMark

PTRF acts as an adipokine contributing to adipocyte dysfunctionality and ectopic lipid deposition

Sergio Perez-Diaz[1] · Maria P. Garcia-Sobreviela[1] · Yolanda Gonzalez-Irazabal[2] · Beatriz Garcia-Rodriguez[2] · Silvia Espina[1,3] · Izaskun Arenaz[4] · Jose M. Arbones-Mainar[1,5]

Abstract

Adipose tissue (AT) expands under obesogenic conditions. Yet, when the growth exceeds a certain limit, AT becomes dysfunctional and surplus lipids start depositing ectopically. Polymerase I and transcription release factor (PTRF) has been proposed as a mechanism leading to a dysfunctional AT by decreasing the adipogenic potential of human adipocyte precursors. However, whether or not PTRF can be secreted by the adipocytes into the bloodstream is not yet known. For this work, PTRF presence was investigated in plasma. We also produced a recombinant PTRF (rPTRF) and examined its impact on the functional interactions between the adipocyte and the hepatocyte in vitro. We demonstrated that PTRF can be found in human plasma, and is at least in part, carried by exosomes. In vitro treatment with rPTRF increased the hypertrophy and senescence of 3T3-L1 adipocytes. In turn, those rPTRF-treated adipocytes increased lipid accumulation in hepatocytes. Lastly, we found a positive correlation between circulating PTRF and the concentration of PTRF in the visceral fat depot. All these findings point toward the presence of an enlarged and dysfunctional visceral adipose tissue which secretes PTRF. This circulating PTRF behaves as an adipokine and may partially contribute to the well-known detrimental effects of visceral fat accumulation.

Keywords Adipose · Cavin-1 · Senescence · Visceral fat

✉ Jose M. Arbones-Mainar
jmarbones.iacs@aragon.es; https://www.adipofat.com

1 Adipocyte and Fat Biology Laboratory (AdipoFat), Unidad de Investigación Traslacional, Instituto Aragonés de Ciencias de la Salud (IACS), Instituto de Investigación Sanitaria (IIS) Aragón, Hospital Universitario Miguel Servet, Isabel la Católica, 1-3, 50009 Zaragoza, Spain

2 Servicio de Bioquímica Clínica, Hospital Universitario Miguel Servet, Zaragoza, Spain

3 Servicio de Aparato Digestivo, Hospital Universitario Miguel Servet, Zaragoza, Spain

4 Biobanco del Sistema de Salud de Aragón, Instituto Aragonés de Ciencias de la Salud (IACS), Zaragoza, Spain

5 CIBER Fisiopatología Obesidad y Nutrición (CIBERObn), Instituto Salud Carlos III, Madrid, Spain

Introduction

The adipose tissue (AT) is a plastic endocrine organ, able to expand and contract in response to different nutritional and metabolic cues. Under obesogenic conditions the AT expands, as the accumulation of triglycerides in the AT is a safe way to store energy surplus. However, when adipose tissue growth exceeds a certain limit, metabolic complications may develop [22]. Some of those complications stem from the ectopic deposition of lipids in tissues such as the muscle, liver, or the omentum [13]. Polymerase I and transcription release factor (PTRF) production by the adipocytes has been proposed as a mechanism leading to a dysfunctional AT [16]. In a previous work, we found an upregulated expression of the PTRF associated with senescence and decreased adipogenic potential of human adipocyte precursors [15].

PTRF is considered a intracellular protein [10]. Yet, in the present work, we found PTRF in the bloodstream of human subjects free of cancer and other chronic diseases, and investigated its effects on adipocytes in vitro. For this, PTRF levels were measured in plasma, as well as both the subcutaneous

Springer

and visceral AT of obese individuals. Moreover, we produced a recombinant PTRF (rPTRF) and examined its impact on the functional interactions between the adipocyte and the hepatocyte in vitro. These studies demonstrated that the visceral AT produces more PTRF than the subcutaneous AT in obese individuals. This work also showed that PTRF is critical for the adipocytes's metabolic responses in vitro and that rPTRF-treated adipocytes increased lipid accumulation in hepatocytes.

Material and methods

Production of recombinant-PTRF

The full-length *Mus musculus* Ptrf cDNA fused with a six histidine tail (C-His) sequence and cloned into the pReceiver expression vector was purchased from Genecopoeia (#EX-Mm04800-B3. Genecopoeia Rockville, MD, USA). Six nanograms of the expression vector were transferred by heat shock to 25 μl (1–7 × 10^6 colony forming units) of competent E.coli, BL21 (DE3)-plysS donated by Olga Abian (Institute of Biocomputation and Physics of Complex Systems, Universidad de Zaragoza, Zaragoza, Spain). The mixture was incubated 30 min on ice, and then 60 s at 42 °C and 2 min back on ice. The transformed cells were maintained in a steady shaking in a 37 °C incubator with 1 ml 2xYT medium for 30 min. Then, 20 μl of the medium were plated in a LB agar supplemented with ampicillin. The plates were incubated in a 37 °C incubator overnight. Each resultant colony was grown in a LB ampicillin medium until reached 0.6 of optical density measured at 600 nm. Then, the expression of the rPTRF was induced with the Overnight ExpressTM Auto-induction System (Novagen, Madison, WI, USA) according to the manufacturer's instructions.

Purification of recombinant rPTRF

Bacteria were collected by centrifugation, 10,000×g for 10 min. The pellet was resuspended with lysis buffer at pH = 8 (50 mM NaH2PO4, 300 mM NaCl, and 10 mM imidazole (#A9978, Sigma-Aldrich, Madrid, Spain)) and the produced rPTRF released by sonication (10 × 15 s bursts at 100 W with 10 s on ice cooling). The lysate was centrifuged and the cleared-supernatant loaded into nickel-conjugated agarose column, Ni-NTA agarose (#1018244, QIAGEN, Valencia, CA, USA). The flow-through was discarded and the column washed to remove nonspecific bindings with wash buffer at pH = 8 (50 mM NaH2PO4, 300 mM NaCl, and 20 mM imidazole). To obtain the rPTRF, we used a gradient of 50 to 200 mM of imidazole-salt buffer to competitively elute the bound polyhistidine residues. One hundred thirty-five elution fractions of 200 μl were collected. The amount of protein present in each fraction was examined the Bio-Rad Protein Assay, based on the method of Bradford (#500-0006, Bio-Rad, Hercules, CA, USA). Selected fractions were assayed for PTRF presence using SDS-PAGE and staining with Coomasie Blue (#161-04-06, Bio-Rad). The observed bands were isolated with a scalpel and the protein content identified by MALDI-TOF (Perkin–Elmer, Boston, USA). The resultant peptides were analyzed by Mascot Data base (Matrix Science) (Proteomics Unit, CIBA. Instituto Aragonés de Ciencias de la Salud, Zaragoza, Spain). For subsequent treatments, the eluted protein was desalted and resuspended in DPBS (#17-512F, Lonza, Switzerland) using Amicon Ultra 15 filters (Merck-Millipore, Darmstadt, Germany) following the provided protocol by the manufacturer. Finally the rPTRF was filtered through a 0.2-μm filter (Thermo Fisher Scientific, San Jose, CA, USA) and frozen until ready to use.

Cell culture, treatments, and metabolite measurements

The 3T3-L1 cells (ATCC, Rockville, MD, USA) were maintained in high-glucose Dulbecco's modified Eagle's medium (DMEM, Lonza) supplemented with 10% of fetal bovine serum (FBS, Lonza) in normoxia conditions, 37 °C and 5% of CO2 in humid atmosphere. Two days after confluence, the 3T3L1 were transformed to mature adipocytes as previously described [8]. After 6–8 days post-differentiation, the mature adipocytes were treated with the maintenance medium supplemented with 0, 0.1, and 0.5 μM of rPTRF or following a time course. The content of glucose present in the culture medium was determined following the protocol provided by Beckman Coulter (Glucose OSR6121, Beckman Coulter, Miami, FL, USA). The HepG2 cells (ATCC) were cultured with high-glucose DMEM until confluence. Then, the conditioned media from the treated mature adipocytes were used to supplement the HepG2 for 2 days. The lipid content was measured by staining the cell culture with the lipophilic dye Oil Red O [17]. Microphotographs were taken using an inverted microscope (Motic AE31; Jed Pella, Redding, CA, USA).

Radioactive assays

The free fatty acids and glucose uptake, lipolysis, and de novo lipogenesis were assayed with 0.5 nCi/μl [9,10-3H(N)]-palmitic acid (NET043005MC; Perkin-Elmer), 15 nCi/μl 2-[1,2-3H(N)]-deoxy-D-glucose (NET549250UC, Perkin-Elmer), and 1 nCi/μl [3H]-acetic acid (NET003005MC; Perkin–Elmer), respectively, as described previously [8]. For the glucose uptake, assay cells were sensitized with insulin 0.5 μM (Actrapid, Novo Nordisk, Bagsvaerd, Denmark) for 30 min and then radioisotope was added for 10 min. Finally,

cells were washed with KRPH buffer and lysed with lysis buffer (0.2 N NaOH, 0.1% SDS) [8].

Plasma and adipose tissue samples

Fresh plasma was donated by 17 individuals free of chronic or acute diseases. The AT biopsies were obtained during elective surgeries (bariatric surgery, cholecystectomy, or hernia repair) from the abdominal subcutaneous or visceral (omental) depots [22]. The biopsies were washed, devoid of vascular and connective tissue, and subsequently stored at $-80\,°C$ in cryopreservation vials. This study was approved by our local Institutional Review Board, the Comité de Ética de la Investigación de la Comunidad de Aragón (CEICA), and informed consent was obtained from all participants and/or their legal guardians.

Isolation of extracellular vesicles

For the isolation of extracellular vesicles (EV) from plasma, we followed the protocol provided by Théry et al. [20]. Blood samples (2 ml) were drawn from three donors free of chronic or acute diseases using EDTA tubes (BD Vacutainer K2E, Becton Dickinson, Plymouth, UK). Next, the EDTA tubes underwent a series of centrifugation steps; first, cellular debris was removed by centrifugation ($1500 \times g$ for 15 min at room temperature in a Eppendorf 5810R; Hamburg, Germany). Next, the supernatants were centrifuged $2000 \times g$ for 30 min at 4 °C and then $12{,}000 \times g$ for 45 min at 4 °C. Finally, the supernatants were ultra-centrifuged ($110{,}000 \times g$ for 120 min at 4 °C, Sorval WX Ultra 100, Thermo Scientific, Asheville, NC, USA). The pellets were resuspended in 1 ml of DPBS and washed two times by ultra-centrifugation, $110{,}000 \times g$ for 60 min at 4 °C. At last, the pellets were solubilized with 100 µl of DPBS.

Transmission electron microscopy

Twenty microliters of isolated EV were spotted onto carbon grids. Each grid was incubated with 2% uranyl acetate (#6159-44-0, Sigma-Aldrich) on water for 2 min in the dark. The sections were examined under a JEOL 1010 (JEOL Ltd., Tokyo, Japan) transmission electron microscope. Images were captured on the Unit of Electronic Microscopy and Biological Systems, Faculty of Medicine, Universidad de Zaragoza, Zaragoza, Spain.

Immunodetection of proteins

Cultured cells were lysed with 100 µl of RIPA (50 mM TRIS, 150 mM NaCl, 1% Igepal (#I8896, Sigma-Aldrich), 0.5% sodium deoxycholate (#49647, Sigma-Aldrich), and 0.01%

de SDS (#BP-166-100, Thermo Fisher Scientific); pH = 8) per 10 cm^3 plate. A cell scraper was used to pool the cell lysate into vials. Likewise, biopsies of AT were mechanically lysed with RIPA buffer in glass potter elvehjem homogenizer. Lysates were then centrifuged for 5 min (150,000 rpm, 4 °C). The pellets were discarded and the protein concentration in supernatants was measured using the Pierce BCA Protein Assay (Thermo Fisher Scientific). Diluted plasma, cell lysates, and EV were subjected to 10% SDS-PAGE, transferred onto PVDF membranes (#10600023, GE Healthcare LifeScience, Germany) and subsequently blocked with 5% skimmed milk. The immunodetection against specific targets were carried out using the following antibodies: PTRF (sc-133934), Caveolin-1 (sc-894), His-tag (sc-803), and Actin (sc-1615; Santa Cruz Biotechnology, Santa Cruz, CA, USA). The signal was increased using the appropriate secondary antibodies. Membranes were exposed to enhanced chemiluminiscent films Novex ECL Chemiluminescent Substrate Reagent (Thermo Fisher Scientific) and analyzed using Image-J (National Institute of Health, Beteshda, MD, USA).

PTRF content in plasma and adipose tissues were quantified by an antigen capture enzyme-linked immunosorbent assay (ELISA), using a 1:2500 dilution of the abovementioned PTRF antibody as previously described [4].

Gene expression

Total RNA was isolated using TRizol Reagent (#T9424, Sigma-Aldrich) and treated with DNAse (#AM2238, Thermo Fisher Scientific) as previously described. Subsequently, the RNA was retrotranscribed to cDNA (#4374966, Thermo Fisher Scientific). The target genes were amplified using specific primers and measured with SYBRgreen I (#4472908, Thermo Fisher Scientific) in a StepOnePlus thermocyler (Thermo Fisher Scientific). Gene expression was calculated by the ddCT method 25 with either actin or A-FABP as housekeeping genes.

Statistical analysis

Results are expressed as mean ± SEM. Every assay was conducted at least in two independent experiments. Pairwise group comparisons were calculated using Student's t test for Gaussian-distributed variables and Mann–Whitney U test for non-Gaussian-distributed data. The p value for trend was computed from the Pearson test to investigate whether or not the responses systematically increase or decrease over the levels of the factor variable (rPTRF dose). The statistical analysis was performed using R version 3.1.3 (http://www.r-project.org) and the level of significance was set at 0.05.

Results

PTRF is present in the bloodstream and associates with exosomes

Western blot analysis revealed that PTRF was present in human serum (Fig. 1b). Next, we isolated exosomes from the plasma of three individuals free of cancer or any chronic disease. Transmission electron microscopy (TEM) imaging showed the exosomes as a ring-shaped structure of no more than 150 nm with the typical optical density of a lipid bilayer (Fig. 1a). To test the presence of PTRF in these extracellular vesicles, a specific antibody was used for the immunodetection of PTRF by Western blot. Figure 1b shows the results of an autoradiographic film in

which we confirmed that this circulating PTRF was, at least partly, carried by exosomes.

PTRF is transported into the 3T3-L1-derived adipocytes in a time-dependent fashion

After demonstrating the presence of PTRF in plasma, we wondered whether circulating PTRF may be taken up by the adipocytes. We produced a recombinant murine PTRF (rPTRF) with a histidine tail as described in material and methods and used it to supplement cultured 3T3-L1-derived adipocytes. Thus, 0.5 μM rPTRF was added to the culture medium and the adipocytes were collected at 10, 20, and 40 min post-loading. Figure 1c illustrates (1) that the rPTRF remained in the
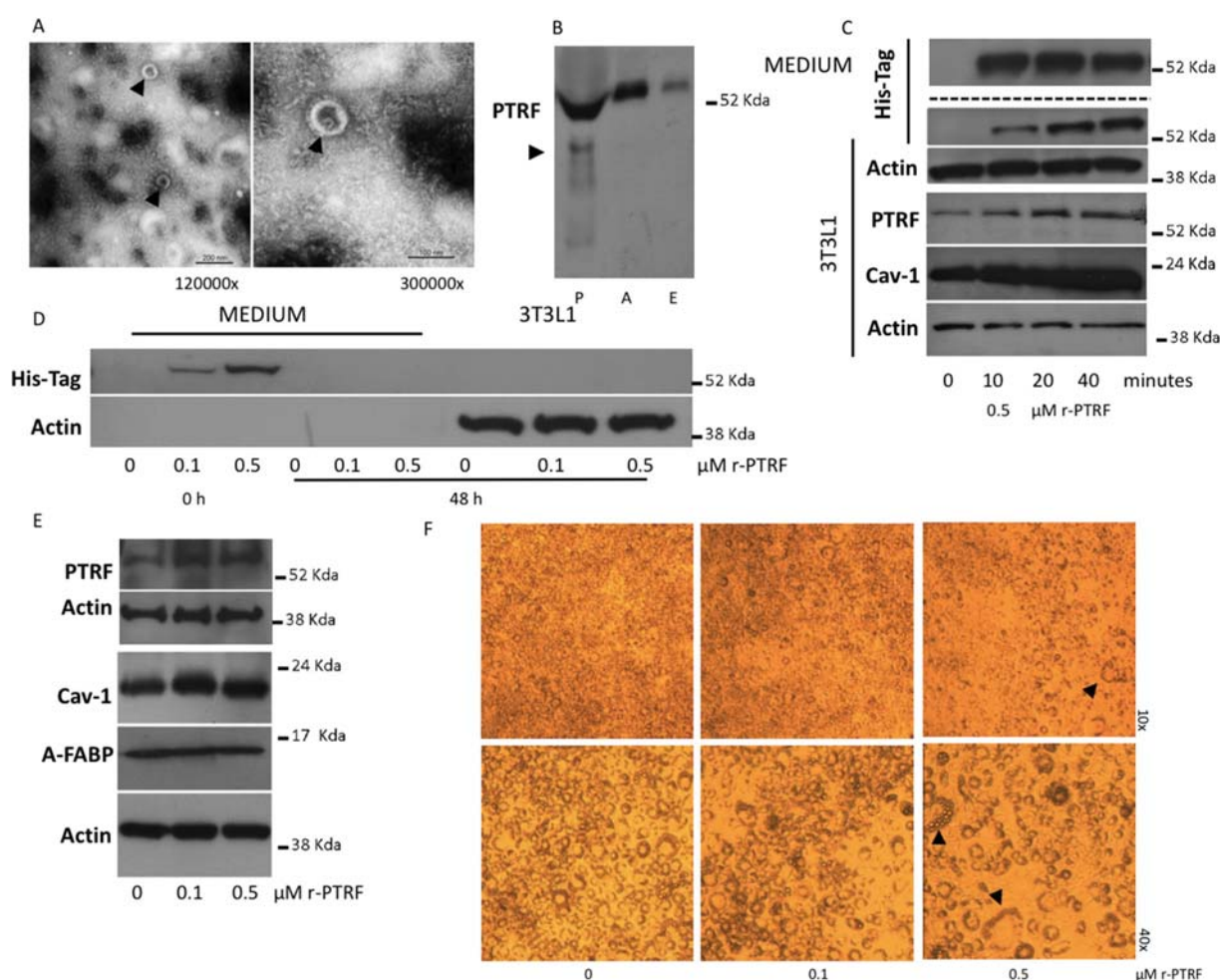

Fig. 1 PTRF is a circulating protein and associates to exosomes. **a** Representative transmission electron micro-photography showing the characteristic spherical shape and the size of exosomes (arrows). **b** Western blot analysis of PTRF in human plasma; P, 3T3L1-derived adipocytes as positive control; A, and exosomes isolated from human plasma, as described in material and methods; E, arrow indicates the size of truncated PTRF. 3T3L1 cells were differentiated into adipocytes and supplemented with 0.5 μM of recombinant PTRF (rPTRF) for either 0, 10, 20, and 40 min. **c** Immunodetection of the histidine tag (His-Tag), PTRF, and Cav-1 in lysated adipocytes and in the rPTRF-supplemented

culture media. **d** Immunodetection of the His-tag in the culture medium at the baseline and after 48 h, as well as His-tag taken up by the adipocytes 48 h post-suplementation with rPTRF. In another set of experiments 3T3L1-derived adipocytes were treated with either 0, 0.1, or 0.5 μM of rPTRF for 48 h. **e** Immunodetection of PTRF, Cav-1, and A-FABP in the whole lysated adipocytes. **f** Representative microphotographies of the treated adipocytes. Arrows point to hypertrophied adipocytes. Western blot images are the most representative of at least two independent experiments and were cropped and obtained under same experimental conditions

culture medium without any degradation or proteolysis and (2) the recombinant protein was internalized by the adipocytes, as the histidine tail signal belonging to the rPTRF appeared inside the cells as early as 10 min post-supplementation. This signal further increased by 80% and a 150% at 20 and 40 min, respectively, suggesting an active transport into the cell. Likewise, rPTRF supplementation produced a concomitant increase in the main components of the caveolae, the endogenous PTRF and Caveolin-1, by 150 and 300%, respectively when compared to the untreated control (Fig. 1c).

rPTRF is rapidly processed inside adipocytes

Knowing the ability of adipocytes to internalize rPTRF from the medium, we investigated whether this soluble rPTRF would have any effect on the adipocyte's functionality. We firstly supplemented the adipocyte culture with 0.5 μM rPTRF for 8 h. Western blot analysis of the treated adipocytes showed a 60% decreased histidine signal and a 70% increased total PTRF levels (endogenous + recombinant + truncated forms) after 8 h, indicating some type of short-term processing of rPTRF within the adipocyte (Supplemental Fig. 1). We next sought to investigate some delayed consequences of rPTRF supplementation. To that end, we treated mature adipocytes with 0, 0.1, and 0.5 μM rPTRF for 48 h to test for some medium-term PTRF effects. Upon rPTRF treatment, proteins and RNA were isolated from adipocytes. Unexpectedly, adipocytes no longer signaled the histidine tail after 48 h of exposure to different concentrations of rPTRF (Fig. 1d). Concomitantly, when compared to their untreated counterparts, the adipocytes treated with 0.1 and 0.5 μM rPTRF increased the expression of PTRF by 50% at both the protein (Fig. 1e) and the mRNA levels (100 ± 4.8, 143 ± 3.4, and 155 ± 4.2 for the adipocytes treated with 0, 0.1, and 0.5 μM rPTRF, respectively. $p < 0.001$ for both treated groups). Simultaneous to the sustained rise in endogenous PTRF, there was an increase of caveolin-1 by 40 and 75% in the groups treated with 0.1 and 0.5 μM rPTRF respectively, when compared to untreated cells (Fig. 1e). Some adipocyte-differentiation markers were also measured, such as adipocyte fatty acid binding protein (A-FABP) and PPARγ (Fig. 1e), which did not change significantly upon treatment with 0.5 μM rPTRF (not shown). However, we did observe how the treatment with rPTRF produced enlarged adipocytes (Fig. 1f).

Treatment with rPTRF modified glucose uptake

We next went on to test whether treatment with rPTRF had any effect on adipocyte functionality. Specifically, we investigated the glucose handling by the 3T3-L1 adipocytes, as this substrate is the main source for de novo triglyceride synthesis in vitro. Firstly, we measured basal consumption of glucose by the adipocytes. Cultures treated with 0.1 and 0.5 μM rPTRF reduced the glucose in the medium by 15% ($p = 0.014$) and

20% ($p < 0.001$) more than the control, respectively (Fig. 2a). We then measured the cells' ability to take up glucose in response to insulin upon rPTRF supplementation. For this, we use radiolabelled 2-deoxyglucose (2DG) and insulin. In basal conditions (no insulin present), adipocytes took up 10 and 40% ($p = 0.028$) more radioactive 2DG when treated with 0.1 and 0.5 μM rPTRF, respectively, compared to untreated adipocytes. When the cells were stimulated with insulin, uptake of 2DG was greater than basal conditions, yet independent of rPTRF treatment (Fig. 2b). The ratios between 2DG captured after insulin stimulation and 2DG taken up without stimulation were calculated as surrogate marker of insulin sensitivity. These ratios ranged from three in the control group (the largest insulin response) to 2.2 and 1.7 in those adipocytes treated with 0.1 and 0.5 μM of rPTRF, respectively ($p = 0.034$ for the difference between control and the group treated with 0.5 μM of rPTRF). Then, we measured the expression levels of the insulin-dependent (GLUT4) and insulin-independent (GLUT1) glucose transporters, as well as the hexokinase II (HK2). Whereas GLUT4 mRNA levels did not change upon rPTRF supplementation, GLUT1 increased by 40 and 90% in the groups treated with 0.1 and 0.5 μM rPTRF, compared to control adipocytes ($p = 0.03$ for the difference between both rPTRF-treated vs control groups) (Fig. 2c). This finding might explain, at least partially, why the expression of HK2, the kinase responsible for phosphorylating glucose, was significantly increased by 40% ($p = 0.023$) and 55% ($p = 0.029$) in the groups treated with 0.1 and 0.5 μM rPTRF (Fig. 2d). All the above would suggest a greater reliance on glucose of the rPTRF-treated adipocytes.

Treatment with rPTRF altered de novo lipogenesis

The primary function of the adipocyte is to store lipids as triglycerides, with glucose being the main substrate for its synthesis by de novo lipogenesis. We did not observe differences in the mRNA levels of the acetyl-CoA Carboxylase α (ACACA) upon rPTRF treatment (not shown). To test their lipogenic capacity, we loaded overnight the adipocytes with radioactively labeled acetate. Subsequently, the acetate incorporated into the lipid fraction was measured in scintillation counter. As occurred with ACACA expression, no changes were observed regarding acetate incorporation into the lipid pool (23.21 ± 2.4, 26.36 ± 2.5, 25.7 ± 2.6 CPM for the groups treated with 0, 0.1, and 0.5 μM rPTRF, respectively). The mismatch observed between glucose uptake and de novo synthesis of captured fatty acids made us wonder about the ultimate fate of glucose. Glucose is the energy source par excellence and when captured by the adipocyte is rapidly phosphorylated by hexokinases entering the glycolysis and generating pyruvate.
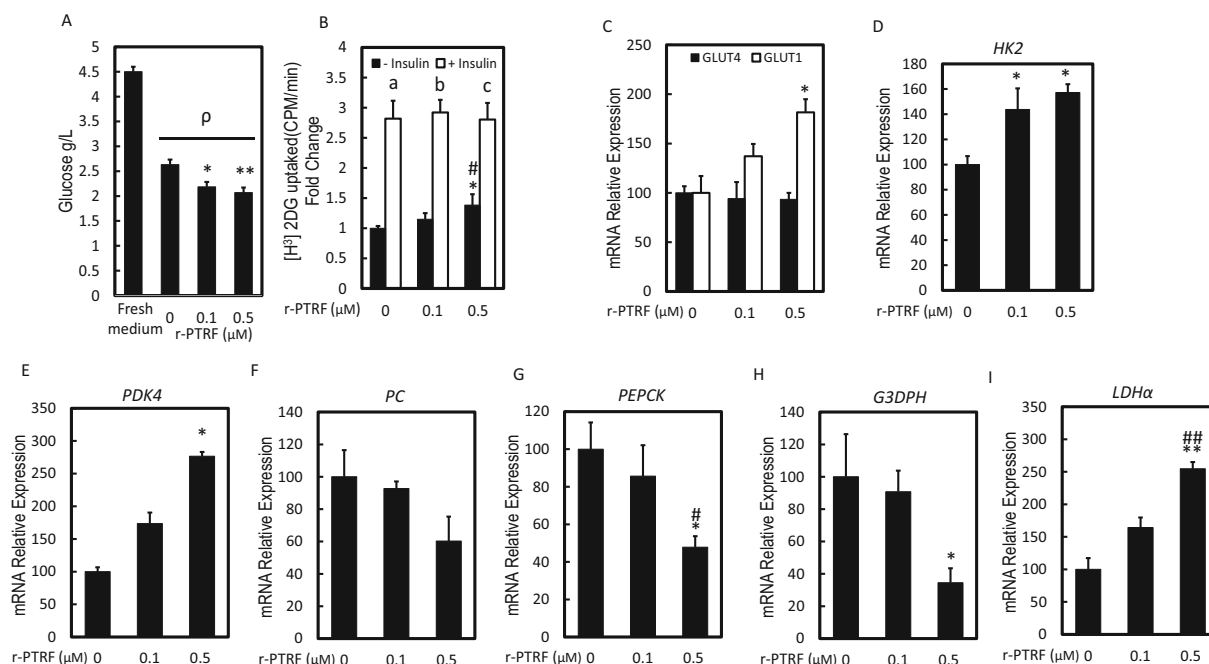
Fig. 2 rPTRF increases basal glucose uptake. 3T3L1-derived adipocytes were treated with either 0, 0.1, or 0,5 μM of rPTRF for 48 h. **a** Concentration of glucose in the culture media after rPTRF treatments. **b** [H3]-2DG uptake assay with (+) and without (-) 0.5 μM insulin for 10 min. mRNA levels of selected genes normalized with β-actin expression: **c** Glucose receptors GLUT1 and GLUT4. **d** Hexokinase II. **e** Pyruvate dehydrogenase kinase 4. **f** Pyruvate carboxylase. **g** Phosphoenolpyruvate carboxykinase. **h** Glyceraldehyde 3-phosphate dehydrogenase. **i** Lactate dehydrogenase alpha. Bars represent mean ± SEM. p, $p < 0.05$ for the differences vs. fresh medium. *$p < 0.05$ and **$p < 0.01$, differences between control (0) and treated groups (0.1 and 0.5 μM r-PTRF). #$p < 0.05$ and ##$p < 0.01$ for the differences within treatment groups (0.1 vs. 0.5 μM r-PTRF)

Fundamental in the metabolism of glucose and fatty acids is the reaction carried out by the PDH by catalyzing the glucose transformation to pyruvate. This reaction is regulated by the pyruvate dehydrogenase kinase 4 (PDK4), which blocks the synthesis of acetyl-CoA by phosphorylation of PDH. Compared to untreated adipocytes, these treated with 0.1 and 0.5 μM rPTRF increased 40 and 125% ($p = 0.044$) expression of PDK4, respectively (Fig. 2e). Blocking the synthesis of acetyl-CoA likely produced an accumulation of pyruvate within the adipocyte. This pyruvate might still enter the TCA bypassing the blockade of PDK4 by carboxylation in oxalacetate by the enzyme pyruvate carboxylase (PC). Yet, we did not find any change in its expression levels upon rPTRF tretament (Fig. 2f). Pyruvate may also be directed toward glycerol from phosphoenolpyruvate. Again, this fate may be ruled out as the expression of machinery responsible for glyceroneogenesis was decreased in the adipocytes treated with rPTRF. Thus, mRNA levels of phosphoenolpyruvate carboxykinase (PEPCK) which catalyzes the reaction of oxalacetate to phosphonenolpyruvate and glycerol 3 phosphate deshydrogrenase (G3PD), responsible for catalyzing the transformation of dihydroxyacetone phosphate into glycerol 3 phosphate were reduced by 60% ($p = 0.0067$) and 80% ($p = 0.042$), respectively, when

adipocytes were treated with 0.5 μM rPTRF (Fig. 2g, h). Alternatively, pyruvate can be reduced to lactate by the action of lactate dehydrogenase α (LDHA). We then determined the expression of this enzyme and found a dramatic increase of 60 ($p = 0.004$) and 150% ($p < 0.001$) in its mRNA levels when the adipocytes were treated with 0.1 and 0.5 μM rPTRF, respectively (Fig. 2i).

Treatment with rPTRF resulted in an increase in dysfunctional adipocyte markers

Hypertrophy in the adipocytes may lead to adipocyte dysfunction [12], and this phenomenon might manifest itself as, among others, increased cellular senescence and altered adipokine secretion. We measured the p16 gene expression, involved in tissue aging, and p53, a nuclear factor involved in cell survival and senescence [5]. Although no significant differences in pairwise comparisons were observed in the p16 mRNA levels among treatment groups, we did find a significant trend ($p = 0.03$) toward augmented gene expression as rPTRF increased (Fig. 3a). Likewise, p53 appeared upregulated by 150% ($p = 0.01$), respectively, in adipocytes treated with 0.5 μM rPTRF (Fig. 3b).

Fig. 3 rPTRF disrupts adipogenesis in vitro. 3T3L1 cells were differentiated into adipocytes and treated with either 0, 0.1, or 0,5 μM of rPTRF for 48 h. mRNA levels of **a** p16 and **b** p53 normalized with β-actin. **c** Immunodetection of adiponectin in the culture medium after rPTRF treatments. Bars represent mean ± SEM. **$p < 0.01$, differences between control (0) and treated (0.1 and 0.5 μM r-PTRF). $^{#}p < 0.05$, differences between the group 0.1 and 0.5 μM r-PTRF. Western blot images were cropped and obtained under same experimental conditions
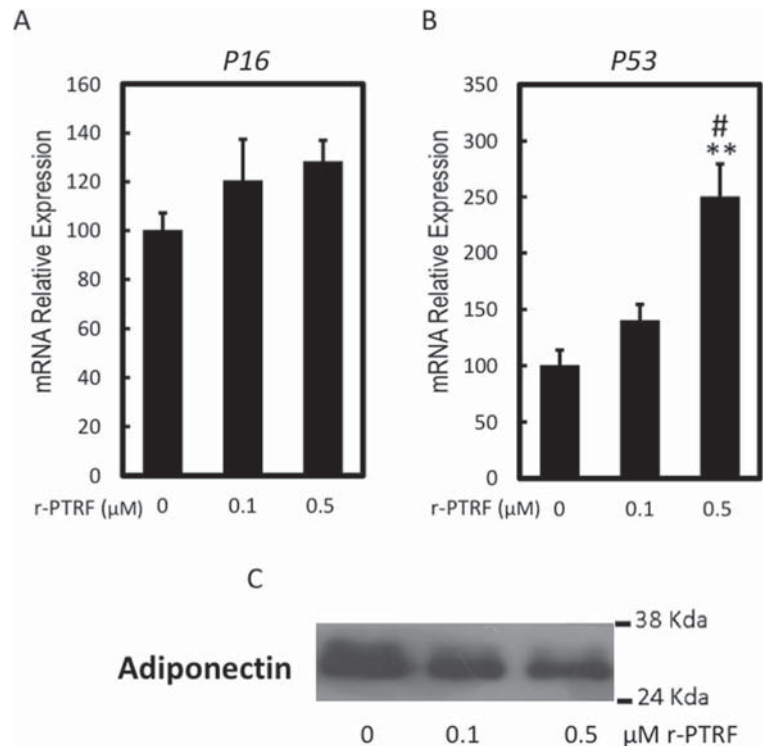
Adiponectin is an important as marker of adipocyte health status. Culture media were collected and the secreted adiponectin was immunodetected. As Fig. 3c illustrates, the media of adipocytes treated with 0.1 and 0.5 rPTRF contained 30 and 50% less adiponectin, respectively, than the control group.

Adipocytes treated with rPTRF promoted lipid accumulation in HEPG2

Considering the detrimental effects of the rPTRF and the endocrine role the adipocytes, we hypothesized that those dysfunctional adipocytes might result in whole body metabolic alterations. Ectopic deposition of fat in the liver is a key feature in the progression of complications associated with obesity [3]. To mimic in vitro the adipocyte-hepatocyte axis HEPG2 hepatocytes were exposed during 48 h to the conditioned media generated by 3T3-L1 adipocytes treated with the different concentrations of rPTRF. De novo lipogenesis in the HEPG2 cells was then measured as described in material and methods. HEPG2 cells conditioned 48 h with the medium from the adipocytes treated with 0.1 and 0.5 μM rPTRF increased the fatty acid synthesis by 40% ($p = 0.031$) and 100% ($p = 0.006$), respectively, compared to the control group (Fig. 4a). An increase of vacuoles inside the hepatocytes cultured with conditioned medium from treated adipocytes was also observed by microscopy. To investigate the nature of such vacuoles, the HEPG2 cells were stained with Oil Red O.

This lipophilic dye was captured by the observed vacuoles thus, revealing themselves as lipid droplets. The dye was then extracted and the amount of lipids contained within the HEPG2 cells was measured by absorbance. Media from adipocytes treated with 0.1 and 0.5 μM rPTRF increased lipid accumulation in HEPG2 cells by 50 and 125% ($p = 0.017$), respectively (Fig. 4b). To confirm the observed results, we measured the expression of some anabolic enzymes. ACACA was upregulated by 45% ($p = 0.010$) and 77% ($p = 0.002$) and LDH by 8% ($p = 0.4$) and 40% ($p = 0.003$) in those HEPG2 cells treated with conditioned medium from adipocytes which had been supplemented with 0.1 and 0.5 μM rPTRF, respectively (Fig. 4c). Likewise, the lipid receptor CD36 increased its expression by 30% ($p = 0.006$) in the HEPG2 cells cultured with the conditioned medium of adipocytes treated with 0.5 μM rPTRF (Fig. 4c).

Human visceral adipose tissue may be a source of plasma PTRF

The adipose tissue releases many factors of different nature with auto-, para-, and endocrine effects [11]. The high expression of PTRF in the adipose tissue made us wonder whether the adipose tissue might be releasing PTRF into the bloodstream. To do this, we used plasma and adipose tissue biopsies from obese individuals and measured PTRF by an in-house ELISA. With a limited cohort study ($n = 9$ male and 8 female), we found that PTRF protein levels were two times higher in
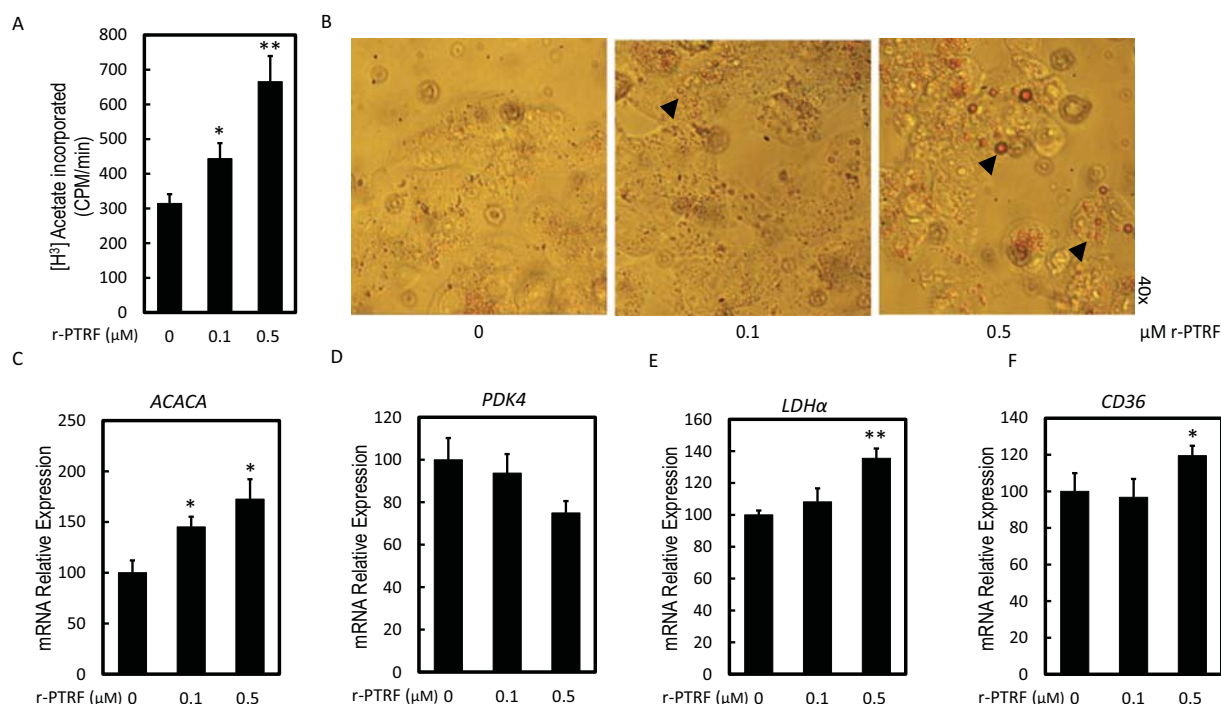
Fig. 4 rPTRF-treated adipocyteconditioned media provokes lipid accumulation in HEPG2 cells. HEPG2 cells were conditioned for 48 h with the medium from 3T3L1-derived adipocytes previously treated with 0.1 and 0.5 μM rPTRF for 48 h. **a** [H3]-acetate incorporated into the cells' lipid fraction depending on the pretreatment of the adipocytes. **b** Microphotographies of the treated HEPG2 cells. Arrows point to lipid droplets within the cells. mRNA levels with β-actin of **c** acetyl-CoA carboxylase alpha, **d** pyruvate dehydrogenase kinase 4, **e** lactate dehydrogenase alpha, and **f** cluster of differentiation 36 in the HEPG2 cells cultured with conditioned adipocyte medium. Values are representative of at least two independent experiments. Bars represent mean ± SEM. *$p < 0.05$ and **$p < 0.01$, differences between control (0) and treated (0.1 and 0.5 μM r-PTRF) cell lines

the visceral (omental) than in the subcutaneous fat tissue (Fig. 5a). Moreover, the relationship between PTRF in the different fat depots and circulating PTRF was determined using correlation analysis (Fig. 5b). The concentration of circulating PTRF was significantly correlated with the amount of PTRF in the visceral adipose tissue but not with the amount of PTRF in the subcutaneous adipose tissue. This strongly suggests the important role of the visceral adipose tissue as source of circulating PTRF.

Discussion

Obesity occurs with an expansion of the adipose tissue to store energy surplus. Increases of adipocyte number (hyperplasia) and adipocyte size (hypertrophy) jointly determine adipose expansion and endogenous PTRF plays an important role in regulating the balance between those two mechanisms [15, 16]. In this work, we showed that PTRF can also be found in human plasma and increases adipocyte hypertrophy and
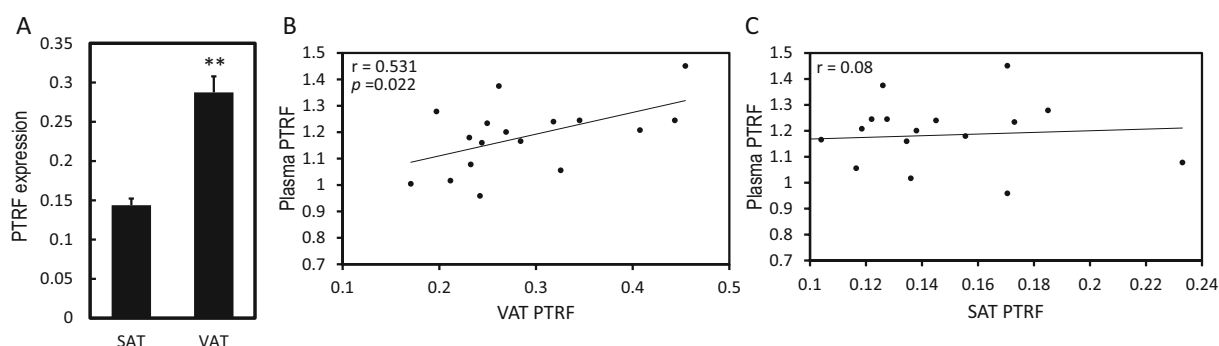

Fig. 5 Circulating PTRF correlates with PTRF levels in visceral adipose tissue. PTRF levels were determined in plasma and adipose depots of obese individuals using an in-house ELISA as described in material and methods. **a** Quantitative detection of PTRF in the subcutaneous (SAT) and visceral (VAT) adipose tissues. Correlation analyses of circulating PTRF and PTRF levels in the visceral (**b**) and the subcutaneous (**c**) adipose tissues. *r*, Pearson correlation coefficient

senescence in vitro. Furthermore, we demonstrated for the first time differences in PTRF production between subcutaneous and visceral fat tissue in obese individuals and also we found a positive correlation between circulating PTRF and the concentration of PTRF in the visceral fat depot.

We, and others, have defined some mechanisms whereby PTRF plays a crucial role in impeding a healthy adipose tissue expansion [1, 15, 16]. For this work, we set out to test whether PTRT might have some endocrine/paracrine influence beyond its effect as endogenous factor. Some studies have already reported the presence of extracellular PTRF in viral capsids [9] and in bladder cancer exosomas [24].Yet, this is the first report showing that PTRF circulates in the blood of individuals free of cancer or any viral disease. Moreover, we also proved that PTRF associated with exosomes. To investigate exogenous PTRF effects on the adipose tissue, we treated adipocytes in vitro with a recombinant murine PTRF (rPTRF). The uptake of rPTRF was sustained over time until its saturation at 1 h post-loading. These phenomena suggest the existence of some system of internalization for rPTRF via facilitated or active transport. PTRF has some domains susceptible to recognize other lipid membranes [2] and thus integrate into caveolae in presence of cholesterol and caveolin-1 [25], although the existence of some yet unknown specific PTRF receptor in the adipocyte cannot be ruled out either. Alternatively, rPTRF transported in exosomes may be also shipped into other target cells using some exosome-specific mechanisms ranging from macro-pinocytosis to membrane fusion, through dependent and independent endocytosis of clathrins. Further investigation is needed as targeting PTRF-internalization mechanism(s) may open new avenues in the treatment of metabolic diseases using cell therapy.

rPTRF's histidine tail gradually disappeared after 48 h. This progressive degradation led us to assume that, once internalized, rPTRF reached the endosome system for its degradation or recycling. We posit that both processes occur simultaneously. PTRF contains some PEST domains associated with proteins that have a short intracellular half-life [2] which some authors have dated in 6 h [21]. Accordingly, we identified by Western blot some truncated forms of PTRF of unknown function (Fig. 1b), likely generated by specific proteolysis. We also detected an increase in the native form of total PTRF suggesting that PTRF recycling is also playing a role in rPTRF processing. This would explain the increase of PTRF and caveolin-1 over time in adipocytes treated with rPTRF. Muller et al. reported that adipocytes can enlarge when treated with certain EV [14] which triggered the expression of some adipogenic genes among which are regulators of caveola expression [19]. We hypothesize that the larger size of the adipocytes treated with rPTRF may be explained by an increased number of caveolae, thus allowing the adipocyte to have a membrane reservoir to rapidly increase cell surface.

rPTRF-treated adipocytes mainly relied on glucose at basal conditions, as we learned from the rapid reduction of glucose from the culture medium, the augmented incorporation of 2DG, as well as the increased expression of HK2, whose over-expression facilitates the assimilation of glucose [7, 23]. Nevertheless, this increased glucose uptake did not translate into an enhanced TG synthesis, increasing only 10% de novo fatty acid synthesis. When we investigated the fate of this glucose, we found a rPTRF-associated increase in the gene expression of PDK4, a metabolic check-point which prevents pyruvate from entering the tricarboxylic acid (TCA) cycle. The adipocyte has then several alternatives for the accumulated pyruvate. Oxaloacetate can be produced from pyruvate through pyruvate carboxylase (PC) and then catalyzed by PEPCK to generate phosphoenolpyruvate as initial steps of glyceroneogenesis (GNG). Yet, we did not find any effect of rPTRF on PC mRNA levels, and when we measured the expression of two key enzymes of the GNG, both PEPCK and G3PDH were decreased in the group treated with the highest concentration of rPTRF. Interestingly, we did find an upregulated expression of LDHA in those cells treated with rPTRF. Although lactate production is classically associated with anaerobic metabolism, its production has been also observed in oxygenated environments rich in glucose [18]. Therefore, the rPTRF-specific increase in glucose uptake resulted in an overexpression of LDHA. Our results are in line with previous reports in which the increase of important caveolar members led to an increased glucose uptake, adipocyte size, and lactate production [6].

In our in vitro liver-adipose tissue model, those HEPG2 supplemented with the conditioned medium from rPTRF-treated adipocytes increased the expression of ACACA and showed augmented lipid droplets within the hepatocytes. Likewise, the HEPG2 treated with this conditioned medium from adipocytes overexpressed the lipid transporter CD36. Herein, we show for the first time how exogenous PTRF produced dysfunctional adipocytes which, in turn, provoked lipid accumulation in a hepatocyte model in vitro. Dysfunctional adipose tissue and fat accumulation in the liver are common features which lead to metabolic syndrome and diabetes. Accordingly, once we proved that PTRF is a circulating protein with endocrine effects, we wondered where this circulating PTRF might be coming from. We found that PTRF levels were 100% higher in visceral than in subcutaneous fat tissue and also found a positive association between the levels of PTRF in visceral adipose and plasma. Indeed, PTRF levels in the visceral depot accounted for an ~30% of the variation of circulating PTRF in obese individuals. All these findings point toward the presence of an enlarged and dysfunctional visceral adipose tissue which secretes PTRF into the circulation. This circulating PTRF may partially contribute to the well-known detrimental effects of visceral fat accumulation.

Compliance with ethical standards

This study was approved by our local Institutional Review Board, the Comité de Ética de la Investigación de la Comunidad de Aragón (CEICA), and informed consent was obtained from all participants and/or their legal guardians.

Conflict of interest The authors declare that they have no conflict of interest.

References

1. Aboulaich N, Chui PC, Asara JM, Flier JS, Maratos-Flier E (2011) Polymerase I and transcript release factor regulates lipolysis via a phosphorylation-dependent mechanism. Diabetes 60:757–765. https://doi.org/10.2337/db10-0744

2. Aboulaich N, Vainonen JP, Strålfors P, Vener AV (2004) Vectorial proteomics reveal targeting, phosphorylation and specific fragmentation of polymerase I and transcript release factor (PTRF) at the surface of caveolae in human adipocytes. Biochem J 383:237–248. https://doi.org/10.1042/BJ20040647

3. Angulo P (2002) Nonalcoholic fatty liver disease. N Engl J Med 346:1221–1231

4. Arbonés-Mainar JM, Navarro MA, Acín S, Guzmán MA, Arnal C, Surra JC, Carnicer R, Roche HM, Osada J (2006) Trans-10, cis-12- and cis-9, trans-11-conjugated linoleic acid isomers selectively modify HDL-apolipoprotein composition in apolipoprotein E knockout mice. J Nutr 136:353–359

5. Baker DJ, Wijshake T, Tchkonia T, LeBrasseur NK, Childs BG, van de Sluis B, Kirkland JL, van Deursen JM (2011) Clearance of p16Ink4a-positive senescent cells delays ageing-associated disorders. Nature 479:232–236. https://doi.org/10.1038/nature10600

6. Briand N, Prado C, Mabilleau G, Lasnier F, Le Lièpvre X, Covington JD, Ravussin E, Le Lay S, Dugail I (2014) Caveolin-1 expression and cavin stability regulate caveolae dynamics in adipocyte lipid store fluctuation. Diabetes 63:4032–4044

7. Fueger PT, Hess HS, Posey KA, Bracy DP, Pencek RR, Charron MJ, Wasserman DH (2004) Control of exercise-stimulated muscle glucose uptake by GLUT4 is dependent on glucose phosphorylation capacity in the conscious mouse. J Biol Chem 279:50956–50961

8. Gamundi-Segura S, Serna J, Oehninger S, Horcajadas JA, Arbones-Mainar JM (2015) Effects of adipocyte-secreted factors on decidualized endometrial cells: modulation of endometrial receptivity in vitro. J Physiol Biochem 71:537–546. https://doi.org/10.1007/s13105-015-0393-0

9. He J, Zheng Y-W, Lin Y-F, Mi S, Qin X-W, Weng S-P, He J-G, Guo C-J (2016) Caveolae restrict tiger frog virus release in HepG2 cells and caveolae-associated proteins incorporated into virus particles. Sci Rep 6

10. Hill MM, Bastiani M, Luetterforst R, Kirkham M, Kirkham A, Nixon SJ, Walser P, Abankwa D, Oorschot VMJ, Martin S, Hancock JF, Parton RG (2008) PTRF-Cavin, a conserved cytoplasmic protein required for caveola formation and function. Cell 132:113–124. https://doi.org/10.1016/j.cell.2007.11.042

11. Kershaw EE, Flier JS (2004) Adipose tissue as an endocrine organ. J Clin Endocrinol Metab 89:2548–2556. https://doi.org/10.1210/jc.2004-0395

12. Kim JI, Huh JY, Sohn JH, Choe SS, Lee YS, Lim CY, Jo A, Park SB, Han W, Kim JB (2015) Lipid-overloaded enlarged adipocytes provoke insulin resistance independent of inflammation. Mol Cell Biol 35:1686–1699. https://doi.org/10.1128/MCB.01321-14

13. McGarry JD (2001) Banting lecture 2001: dysregulation of fatty acid metabolism in the etiology of type 2 diabetes. Diabetes 51:7–18. doi: https://doi.org/10.2337/diabetes.51.1.7

14. Müller G, Schneider M, Biemer-Daub G, Wied S (2011) Upregulation of lipid synthesis in small rat adipocytes by microvesicle-associated CD73 from large adipocytes. Obesity 19:1531–1544

15. Perez-Diaz S, Garcia-Rodriguez B, Gonzalez-Irazabal Y, Valero M, Lagos-Lizan J, Arbones-Mainar J (2017) Knock-down of PTRF ameliorates adipocyte differentiation and functionality of human mesenchymal stem cells. Am J Physiol - Cell Physiol 312:C83–C91. https://doi.org/10.1152/ajpcell.00246.2016

16. Perez-Diaz S, Johnson LA, Dekroon RM, Moreno-Navarrete JM, Alzate O, Fernandez-Real JM, Maeda N, Arbones-Mainar JM (2014) Polymerase I and transcript release factor (PTRF) regulates adipocyte differentiation and determines adipose tissue expandability. FASEB J 28:1–11. https://doi.org/10.1096/fj.14-251165

17. Ramirez-Zacarias JL, Castro-Munozledo F, Kuri-Harcuch W (1992) Quantitation of adipose conversion and triglycerides by staining intracytoplasmic lipids with Oil red O. Histochemistry 97:493–497

18. Sabater D, Arriarán S, del Mar Romero M, Agnelli S, Remesar X, Fernández-López JA, Alemany M (2014) Cultured 3T3L1 adipocytes dispose of excess medium glucose as lactate under abundant oxygen availability. Sci Rep 4:3663

19. Tencer L, Burgermeister E, Ebert MP, Liscovitch M (2008) Rosiglitazone induces caveolin-1 by PPARγ-dependent and PPRE-independent mechanisms: the role of EGF receptor signaling and its effect on cancer cell drug resistance. Anticancer Res 28:895–906

20. Théry C, Amigorena S, Raposo G, Clayton A (2006) Isolation and characterization of exosomes from cell culture supernatants and biological fluids. Curr Protoc cell Biol:3–22

21. Tillu VA, Kovtun O, McMahon K-A, Collins BM, Parton RG (2015) A phosphoinositide-binding cluster in cavin1 acts as a molecular sensor for cavin1 degradation. Mol Biol Cell 26:3561–3569

22. Torres-Perez E, Valero M, Garcia-Rodriguez B, Gonzalez-Irazabal Y, Calmarza P, Calvo-Ruata L, Ortega C, Garcia-Sobreviela M, Sanz-Paris A, Artigas J, Lagos J, Arbones-Mainar J (2015) The FAT expandability (FATe) project: biomarkers to determine the limit of expansion and the complications of obesity. Cardiovasc Diabetol 14:40. https://doi.org/10.1186/s12933-015-0203-6

23. Wasserman DH, Kang L, Ayala JE, Fueger PT, Lee-Young RS (2011) The physiological regulation of glucose flux into muscle in vivo. J Exp Biol 214:254–262

24. Welton JL, Khanna S, Giles PJ, Brennan P, Brewis IA, Staffurth J, Mason MD, Clayton A (2010) Proteomic analysis of bladder cancer exosomes. Mol Cell Proteomics mcp–M000063

25. Yamaguchi T, Lu C, Ida L, Yanagisawa K, Usukura J, Cheng J, Hotta N, Shimada Y, Isomura H, Suzuki M (2016) ROR1 sustains caveolae and survival signalling as a scaffold of cavin-1 and caveolin-1. Nat Commun 7